
Journal of Intelligent and Robotic Systems **23:** 331–349, 1998.

Contact Friction Compensation for Robots Using Genetic Learning Algorithms

DER-CHERNG LIAW and JENG-TZE HUANG
Department of Electrical and Control Engineering, National Chiao Tung University, Hsinchu, 30039 Taiwan, R.O.C.; e-mail: dcliaw@cc.nctu.edu.tw

(Received: 1 September 1997; accepted: 21 April 1998)

Abstract. In this paper, the issues of contact friction compensation for constrained robots are presented. The proposed design consists of two loops. The inner loop is for the inverse dynamics control which linearizes the system by canceling nonlinear dynamics, while the outer loop is for friction compensation. Although various models of friction have been proposed in many engineering applications, frictional force can be modeled by the Coulomb friction plus the viscous force. Based on such a model, an on-line genetic algorithm is proposed to learn the friction coefficients for friction model. The friction compensation control input is also implemented in terms of the friction coefficients to cancel the effect of unknown friction. By the guidance of the fitness function, the genetic learning algorithm searches for the best-fit value in a way like the natural surviving laws. Simulation results demonstrate that the proposed on-line genetic algorithm can achieve good friction compensation even under the conditions of measurement noise and system uncertainty. Moreover, the proposed control scheme is also found to be feasible for friction compensation of friction model with Stribeck effect and position-dependent friction model.

Key words: constrained robots, genetic algorithms, learning, friction compensation.

1. Introduction

In recent years, robots have been used to undertake many tasks in automatic factories. These tasks, depending on the interaction between the robot and the environment, can be classified into contact and non-contact tasks [1]. In performing the non-contact tasks, the robot moves freely in space and requires a position control only [1]. However, in general, control of both the positon and the contact force are simultaneously needed to carry out the contact tasks [1–4]. The position/force control of a robot has been studied by many researchers. For instance, a general review can be found in [4].

When the robot is executing a constrained motion, of which the contacted surface is rigid, the movement normal to the surface is apparantly inhibited. This implies that the total independent coordinates can be reduced to benefit the control designs. A modified computed-torque control scheme [5] was proposed to decouple the constrained robot dynamics into a set of linear subsystems via coordinate reduction and inverse dynamics technique, which results in a global tracking of

position and contact force for frictionless contact surface. The results of [5] have been extended to the study of constrained robot motion on a frictional surface [6]. However, the control design of [6] relies on the known exact modeling of the frictional force to fit the requirement of inverse dynamics technique.

For the compensation of unknown contact friction, the high gain control design is commonly used to guarantee the practical stability of robot motion if the bound of the frictional force is provided [7]. Adaptive friction compensation schemes have been proposed to compensate friction in a variety of mechanisms [8, 9]. However, the results were obtained only for the system linearization, which might not be effective for the original nonlinear dynamics. Nonlinear scheme for friction compensation was shown [10] to provide better system performance than linear approach, even if the contact friction is not exactly cancelled. In general, the contact friction is unknown and hard to measure. Fuzzy neural theory has recently been applied to study such an issue [11]. However, it is restricted for learning the Coulomb friction [11].

Contact friction force varies together with applied normal force, relative velocities, surface conditions and so on [12]. Experiments conducted for identifying friction force are off-line in nature and time-consuming. The friction model composed of the Coulomb friction plus the viscous force is adaquate for many engineering applications [12]. Two friction coefficients are required to fully describe the friction force in such a model. In this paper, we will use this model and focus on the study of the contact friction compensation for constrained manipulators.

By emulating the best-to-survive evolution laws of nature genetics, genetic algorithms (GAs) are global searching algorithms capable of rapidly locating suboptimal solutions for difficult problems [13–15]. Basically, GA consists of three fundamental operators: reproduction, crossover, and mutation [14]. Given a solution space to be searched, each possible solution is encoded as a finite-length string first. The genetic algorithm then randomly searches for the solution in such a discretized space repeatedly via the three operators which are guided by a prescribed fitness function aimed to preserve the best among the survivals. Genetic algorithm prevails over conventional optimum schemes, especially in complex, multimodal, and noisy situations since it poses no requirement on the derivatives of the cost functions. Moreover, GAs are more efficient than other random search algorithms for their capability of accumulating the useful information during the process of search. Since the robot system is highly nonlinear and the friction force is known to be discontinuous at the zero velocity, in this paper genetic algorithm is applied to compensate friction for constrained manipulators.

The paper is organized as follows. In Section 2, brief review of equations of motion for constrained robot manipulators as well as the genetic algorithm are given. It is followed by the design of two-loop friction compensator. An example study of two-link planar robot interacting with rough surface is presented in Section 4 to demonstrate the effectiveness of the design. To summarize the main results a conclusion is given in Section 5.

2. Preliminaries

2.1. DYNAMICAL EQUATIONS FOR CONSTRAINED MANIPULATORS

The dynamical equation of an n-joint constrained manipulator, in terms of the joint variables, can be written as (e.g., [3])

$$\mathcal{M}(q)\ddot{q} + \mathcal{H}(q, \dot{q}) = \tau + J^{\mathrm{T}} f, \tag{1}$$

where $q, \dot{q}, \ddot{q}$ denote the $n \times 1$ joint position, velocity, acceleration vectors, respectively; $\mathcal{M}(q)$ is the $n \times n$ symmetric inertia matrix; $\mathcal{H}(q, \dot{q})$ contains the centripetal, Coriolis and gravitational forces; τ is the joint control torque; $J(q)$ is the system's Jacobian matrix; and f is the reaction force vector at the end effector. In this paper, we assume $\mathcal{M}(q)$ is nonsingular in the workspace.

Since both position and force commands are generally given relative to the end effector, it is natural to express the constrained robot dynamics in Cartesian coordinates. Let $X \in R^n$ denote the position vector of the end effector in Cartesian coordinates. By a diffeomorphic coordinate transformation, the dynamical equations for constrained manipulator can then be obtained as (e.g., [3])

$$M(X)\ddot{X} + H(\dot{X}, X) = T + f, \tag{2}$$

where

$$M(X) := \left(J^{\mathrm{T}}\right)^{-1} \mathcal{M} J^{-1}; \qquad H(\dot{X}, X) := \left(J^{\mathrm{T}}\right)^{-1} \mathcal{H} - \left(J^{\mathrm{T}}\right)^{-1} \dot{J} J^{-1} \dot{X};$$
$$T = \left(J^{\mathrm{T}}\right)^{-1} \tau.$$

Moreover, $M(X)$ is nonsingular since $\mathcal{M}(q)$ is nonsingular and the transformation is diffeomorphic.

For constrained robot motion, the force command generally lies along the normal direction of the constraint surface. Without loss of generality, assume the last component of X is along that direction. The position vector can then be expressed as $X = [\xi \ 0]^{\mathrm{T}}$, with $\xi \in R^{n-1}$. Since we consider the issue of sliding friction compensation only, for simplicity, ξ is assumed to contain purely the sliding vector. The contact force is expressed as $f = [f_t \ f_n]^{\mathrm{T}}$ with $f_t \in R^{n-1}$ and $f_n \in R$. Physically, f_t and f_n denote the frictional force and the normal force, respectively. Thus, $M(X)$, $H(\dot{X}, X)$ and T can be expressed as

$$M(\xi) = \begin{bmatrix} M_t(\xi) & M_u(\xi) \\ M_n(\xi) & M_v(\xi) \end{bmatrix}, \quad H(\dot{\xi}, \xi) = \begin{pmatrix} H_t(\dot{\xi}, \xi) \\ H_n(\dot{\xi}, \xi) \end{pmatrix}, \quad T = \begin{pmatrix} T_t \\ T_n \end{pmatrix}, \tag{3}$$

where $M_t(\cdot) \in R^{(n-1)\times(n-1)}$, $M_n(\cdot) \in R^{1\times(n-1)}$, $H_t(\cdot, \cdot) \in R^{n-1}$, $H_n(\cdot, \cdot) \in R$, $T_t \in R^{n-1}$ and $T_n \in R$. Equation (2) can be rewritten as

$$M_t(\xi)\ddot{\xi} + H_t(\dot{\xi}, \xi) = T_t + f_t \tag{4}$$

and

$$M_n(\xi)\ddot{\xi} + H_n(\dot{\xi}, \xi) = T_n + f_n. \tag{5}$$

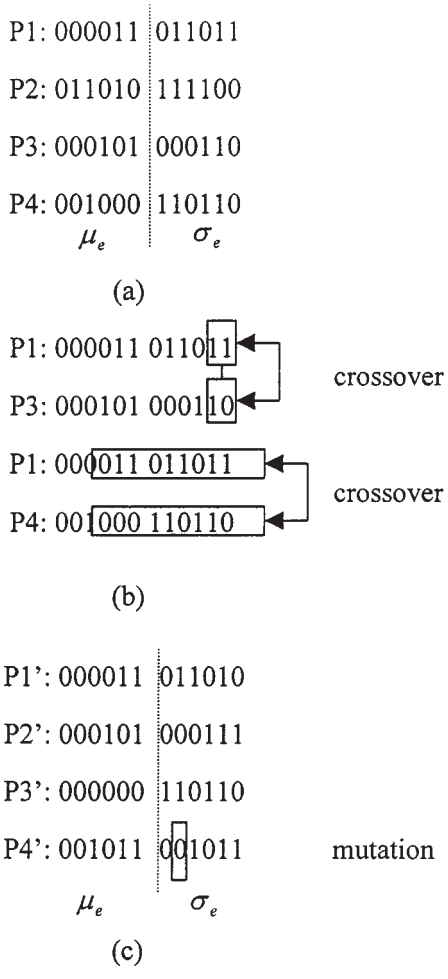

Figure 1. Three operations of GAs: (a) reproduction, (b) crossover, (c) mutation.

Note that the differential Equation (4) describes the free motions on the contacted surface, while Equation (5) can be used to calculate the normal contact force. These equations will be employed in Section 3 to derive the control laws.

2.2. GENETIC ALGORITHMS

In control applications, calculus-based optimization schemes are often employed to seek for the optimal control gains to meet the performance requirements. However, those designs presume the cost functions to be smooth enough. Thus, they might not be applicable to noisy and discontinuous cases. Besides, most of these schemes obtain only the local optima but not the global ones. These drawbacks magnify themselves when the functions are multimodal, discontinuous, or noisy. To solve such problems, random search algorithms have received much attentions for being

immune to those shortcomings. As discussed in [13], pure random search only provides a lower bound for performance since none of the accumulating information is used to guide its search. However, genetic algorithm leads to better results because of its highly guided search and high efficiency.

GAs are global optimization techniques overwhelming the conventional search techniques, especially, when the search space is complicated because of its big size. They simulate the nature evolution which preserves the best among the survivors via a systematic information exchange guided by probabilistic decisions. In a simple genetic algorithm, the solution structure is required to be coded as binary strings. First, random selection of a population of the coded numbers, called the initial population, is initiated. To demonstrate the methodology, an example of initial population with four members, denoted as P1, P2, P3, P4, is shown in Figure 1(a). Genetic algorithm then proceeds iteratively with three consecutive operations: reproduction, crossover, and mutation. Reproduction is a process in which individual strings are copied according to their fitness function values. It means that a string with higher fitness value has higher probability of contributing one or more offsprings in the next generation. The crossover operator then proceeds in two steps: (i) strings are mated randomly; and (ii) mated string couples cross over with crossing site selected randomly. For instance, assume that (P1, P3) and (P1, P4) are selected as mating couples with the crossing site occurring at bit positions 2 and 9, as shown in Figure 1(b). The last operator "mutation" is usually performed on a bit-by-bit basis with small occurring probability. For instance, assume that bit 5 in P4 is mutated. The final result after the crossover and the mutation process is shown in Figure 1(c). New generations go through the three operations again and again until the best-fit solution is found. As discussed in [14], by such an approach, GAs have yielded good results in many practical problems.

3. Controller Designs

In the following, we consider the tracking problem for constrained manipulators moving on a frictional surface. The design consists of two loops. The inner loop is the modified computed-torque control which, linearizing the system by feedback, achieves global stability in tracking the position and the force for frictionless cases. Denote by ξ_{d}, f_n^{d} the desired motion on the constrained surface and the desired normal contact force, respectively. Let e be the position error, i.e., $e = \xi - \xi_{\mathrm{d}}$. According to [5], a modified computed-torque control law for system (4)–(5) can be selected as

$$T_t = M_t(\xi)\left(\ddot{\xi}_{\mathrm{d}} - g_v\dot{e} - g_e e\right) + H_t(\xi, \dot{\xi}) + u \tag{6}$$

and

$$T_n = M_n(\xi)\left(\ddot{\xi}_{\mathrm{d}} - g_v\dot{e} - g_e e\right) + H_n(\xi, \dot{\xi}) - f_n^{\mathrm{d}}, \tag{7}$$

where $g_v, g_e \in R^{(n-1)\times(n-1)}$ denote two diagonal gain matrices with $g_v, g_e > 0$. Here, u is the extra applied control input for friction compensation which will

be designed in Section 3.2 below. Equations (4), (5) in Section 2.1 can now be rewritten as

$$M_t(\xi)\left(\ddot{e} + g_v\dot{e} + g_e e\right) = u + f_t \tag{8}$$

and

$$M_n(\xi)\left(\ddot{e} + g_v\dot{e} + g_e e\right) = f_n - f_n^{\mathrm{d}}. \tag{9}$$

Since $M_t(\xi)$ is nonsigular in the task space and $g_v, g_e > 0$, it is obvious that $e \to 0$ and $f_n \to f_n^{\mathrm{d}}$ as $t \to \infty$ when $f_t = 0$ and the extra control input $u = 0$ [5]. However, when friction $f_t \neq 0$, the extra control force u will be required to cancel the effect of f_t. As presented in [6], high tracking performance can be achieved if the friction is exactly cancelled. However, the friction f_t is generally unknown and is known to be dependent on normal force, sliding velocities, surface conditions and so on. Therefore, on-line identification of friction is required for friction cancellation. In the following, model-based friction compensators will be installed via an on-line genetic learning algorithm for friction compensation. In Section 3.1, the friction models adopted in the study will be briefly reviewed. It is followed by the control algorithm design for friction compensation.

3.1. FRICTION MODELS

It is known that friction occurs at the contacted surface between two mechanical bodies and always opposes to the relative motion. When a robot is carrying out motion on some constrained surface, contact friction may degrade the tracking performance if it is not properly compensated. To understand friction phenomena is a very important issue.

Friction usually occurs in two forms: the static and the dynamic frictions. Using the above defined notations, we can characterize the static and dynamic frictions as follows. First, the static friction is generally characterized by some maximum value, denoted as $f_{\max}$, under which the static state remains, i.e., (e.g., [7])

$$f_t^i = \begin{cases} u^i, & |u^i| < f_{\max} \\ \operatorname{sgn}(u^i) f_{\max}, & |u^i| \geqslant f_{\max} \end{cases} \quad \text{when } \dot{\xi}^i = 0, \tag{10}$$

where $f_{\max}$ is some constant positive scalar, $\dot{\xi}^i$ denotes the ith component of the sliding velocity $\dot{\xi}$, f_t^i and u^i denote the ith components of the friction vector and the tangential applied force, respectively. The dynamic friction is more complicated and has been differently modeled for various applications [12]. Typically, the dynamic friction can be described as

$$f_t^i = -\operatorname{sgn}\left(\dot{\xi}^i\right) f_{\mathrm{slide}}, \tag{11}$$

where f_{slide} represents the magnitude of f_t^i. Note that, in general, f_{slide} is not a constant and is unknown. However, in many engineering applications, f_{slide} can

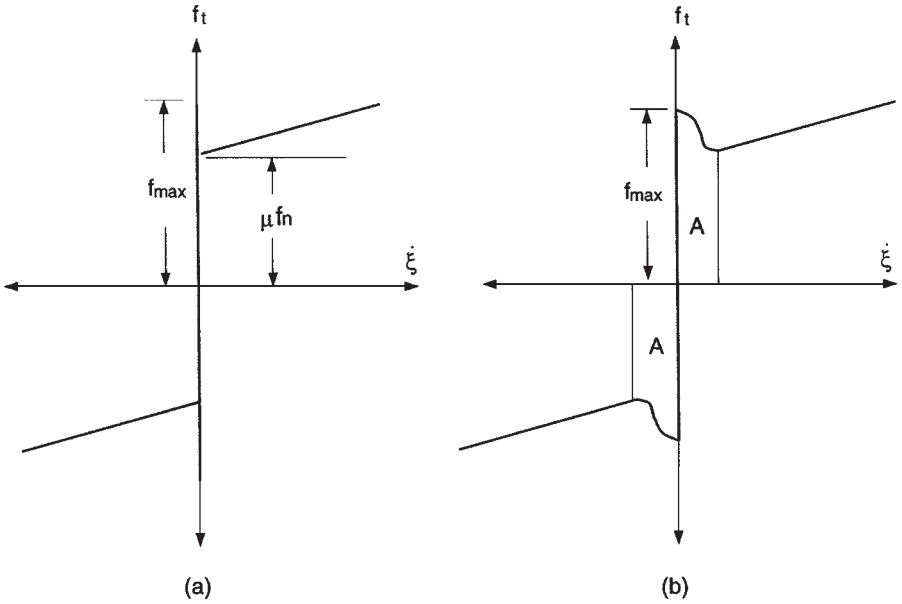

Figure 2. Friction models: (a) Coulomb + viscous, (b) Stribeck effect in region A.

be modeled as the Coulomb friction plus a viscous force [12], as depicted in Figure 2(a). It is known that the Coulomb friction is proportional to the normal force applied to the contact surface, while the viscous force is proportional to the relative velocity of the two bodies. The friction along the $\dot{\xi}_i$ direction can then be written as

$$f_{\text{slide}} = \mu f_n + \sigma \dot{\xi}_i, \tag{12}$$

where μ and σ denote the coefficients of Coulomb friction and viscous force, respectively. Recently, an additional friction phenomenon, the so-called "Stribeck effect", was discovered near the zero velocity [12]. The dynamic friction including the Stribeck curve labeled as A in Figure 2(b), can then be modeled as in [12]

$$f_t^i = -\text{sgn}(\dot{\xi}_i)\left\{\mu f_n^i + \sigma \dot{\xi}^i + c_1 e^{-(\dot{\xi}^i/c_2)^{c_3}}\right\}, \tag{13}$$

where $c_1,\ c_2,\ c_3$ are positive constants. The overall friction function can then be obtained as depicted in Figure 2(b).

In this paper, however, the friction force is assumed to be characterized by Equation (12) and the Stribeck effect is considered as a disturbance. Under such assumption, a best pair of (μ, σ), as in Equation (12), is to be learned for friction compensation. If both μ and σ are exactly estimated, the position and the force errors can then be driven to zero because of exact cancellation of friction. The goal of the next section is to design such a control algorithm via genetic algorithm approach.

3.2. GENETIC LEARNING ALGORITHM DESIGNS FOR FRICTION COMPENSATION

In the following, we assume the friction is composed of the Coulomb friction and the viscous force only. As discussed above, it can be determined by the two coefficients: μ and σ. A genetic-based on-line friction compensator design is proposed in this section to effectively cancel the sliding friction. Here are the details.

From Equations (8), (9), we have

$$M_t\big(\xi(k)\big)\big(\ddot{e}(k) + g_v\dot{e}(k) + g_e e(k)\big) = u(k) + f_t(k) \tag{14}$$

and

$$M_n\big(\xi(k)\big)\big(\ddot{e}(k) + g_v\dot{e}(k) + g_e e(k)\big) = f_n(k) - f_n^{\mathrm{d}}(k), \tag{15}$$

where k denotes the kth sampling time.

Note that the right-hand sides of Equations (14), (15) are the applied forces, while the left-hand sides are the consequences of the applied forces in terms of the kinematic variables. The friction force f_t on the right-hand side is generally unknown and hard to estimate. On the other hand, the kinematics is usually measurable or calculable via suitable sensors. It is clear from Equation (14) that the left-hand side of Equation (14) can provide the information of the difference between the extra control input $u(k)$ and the function $f_t(k)$. Thus, we can transform the friction compensation problem into the friction tracking problem.

In real applications, the acceleration $\ddot{\xi}$ is not easy to measure. A first-order approximation can be adopted to calculate the acceleration as

$$\ddot{\xi}(k) = \big(\dot{\xi}(k) - \dot{\xi}(k-1)\big)/\Delta t, \tag{16}$$

where Δt denotes the sampling period. At the beginning of each sampling time, the friction compensation force $u(k) := \mu_e f_n(k) + \sigma_e\dot{\xi}(k)$ is generated and fed into the robot dynamics, where μ_e and σ_e are randomly assigned. The fitness value with respect to current value of (μ_e, σ_e) is evaluated to create next generation of (μ_e, σ_e). Two errors, the tangential force error $E_t(k) := \|u(k) - f_t(k)\|$ and the normal force error $E^n(k) := \|f_n(k) - f_n^{\mathrm{d}}(k)\|$ are adopted for calculating the fitness function values in this proposed compensator design. As discussed above, they can be approximated by

$$\begin{aligned} E_t(k) \;\approx\; & \big\| M_t(k)\big(\big(\dot{\xi}(k+1) - \dot{\xi}(k)\big)\big/\Delta t - \ddot{\xi}_{\mathrm{d}}(k+1) + g_v\dot{e}(k+1) + \\ & + g_e e(k+1)\big)\big\|, \end{aligned} \tag{17}$$

and

$$\begin{aligned} E_n(k) \;\approx\; & \big\| M_n(k)\big(\big(\dot{\xi}(k+1) - \dot{\xi}(k)\big)\big/\Delta t - \ddot{\xi}(k+1) + g_v\dot{e}(k+1) + \\ & + g_e e(k+1)\big)\big\|. \end{aligned} \tag{18}$$

It should be noted that $E_t(k)$ is approximated by Equation (17) with the kinetic variables measured at the begining of the $(k+1)$th sampling time, i.e., the end of

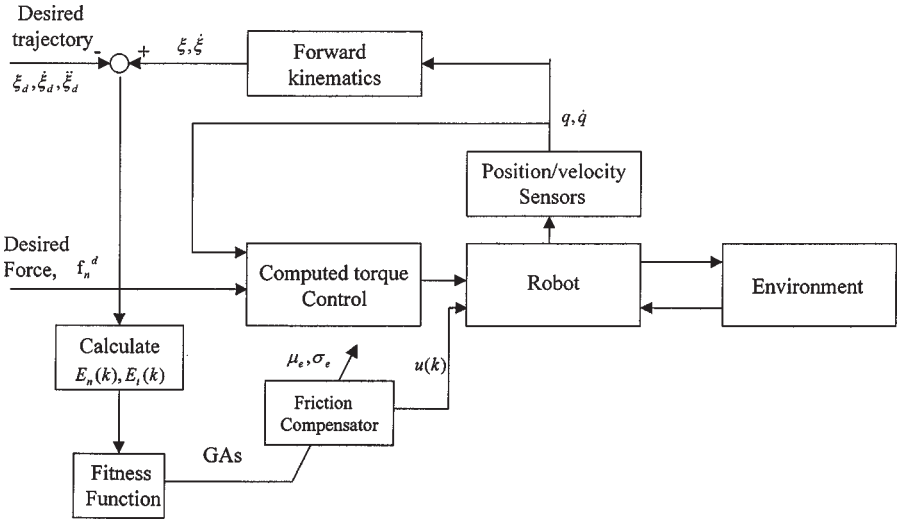

Figure 3. Schematic diagram of the closed loop system.

the kth sampling time. On the other hand, $E_n(k)$ can be exactly calculated when $f_n(k)$ is measured. In other cases, the right-hand side of Equation (17) is a good replica. Intuitively, only $E_t(k)$ is required for justifying the fitness of the estimated pair (μ_e, σ_e). However, uncertainties arising from the calculation of Equation (17), friction modeling and many others always exist in real applications. Therefore, $E_n(k)$ is accompanied as an auxilliary information for the evaluation of the fitness.

Based on these approximations, a properly defined fitness function can then be calculated for the guide of searching process in the genetic algorithms. The fitness function is chosen for this application is

$$F(k) = 0.5 \exp\left(-E_t(k)/\delta_1\right)\left(1 + \exp\left(-E_n(k)/\delta_2\right)\right), \tag{19}$$

where δ_1, δ_2 are constants to be selected for applications.

The whole schematic diagram of our controller is depicted in Figure 3. As discussed previously, the inner-loop computed torque control is used to render the constrained robot dynamics into two orthogonal subsystems as given in Equations (4), (5). The outer loop, the friction compensator installed with an on-line genetic learning algorithm, is used to learn the friction coefficients for canceling the friction force. Detailed implementation of the learning algorithms is presented as follows.

To be processed by the GAs, firstly, the estimated parameters: (μ_e, σ_e) must be coded as finite-length binary strings. Assume N_μ bits are for μ_e and N_σ bits for σ_e. Then, there will be totally $2^{N_\mu + N_\sigma}$ pairs in the search space, denoted as Ω. Initially, N pairs of (μ_e, σ_e) in Ω, called the initial population, are randomly generated. Then each pair of (μ_e, σ_e) in the initial population is assigned a particular sampling interval, during which the estimated pair will be tested to justify its fitness sequentially. As stated previously, this is accomplished by injecting a corresponding compensa-

tion force $u(k)$ into the robot system in the beginning of the kth sampling interval, and evaluating its fitness value defined in Equation (19) at the end of that sampling interval. After N sampling intervals, the testing for the whole initial population will be completed. The next generation will then be produced by performing three consecutive operators: reproduction, crossover, and mutation. Though randomly reproduced, however, as discussed in Section 2, individuals with higher fitness values will have a bigger chance to be selected as parents to generate their own offsprings in the next generation. Therefore, through iterative uses of the genetic operators, new generations with higher fitness values are produced consequently until the near-optimal solution is found.

Denote N the population size. It will clearly consume about $N\Delta t$ seconds for each iteration of the whole process. Therefore, assume that there are N_{gen} generations for a complete learning. The learning period, denoted as T_l (sec), can then be estimated as

$$T_l(\text{sec}) = NN_{\text{gen}}\Delta t. \tag{20}$$

It is noted that the learning rate is proportional to the sampling time. So, higher sampling rate is preferred to provide quick convergence.

4. Numerical Examples

In this section, to demonstrate the validity of our design, a two-joint constrained robot system is used for simulation, as depicted in Figure 4. The dynamical equations for such a system can be found in [3]. Parameters of the manipulator and the control algorithms are given in Tables I and II. Initial conditions of the manipulator are given in Table III. It is known that the inverse dynamics based control methods are quite sensitive to the choice of sampling time [16]. Therefore, the high sampling rate and also high gains, as given in [6], are selected for our simulation as shown in Tables II and III.

The position of the end effector in Cartesian coordinates (x_1, x_2), as can be easily checked in Figure 4, is related to the joint position as follows:

$$x_1 = l_1\sin(q_1) + l_2\sin(q_1 + q_2), \tag{21}$$

$$x_2 = l_1\cos(q_1) + l_2\cos(q_1 + q_2), \tag{22}$$

Table I. Parameters of the manipulator

		Link 1	Link 2	Unit
Arm length	L	0.5	0.4	m
Mass	M	3	2	kg

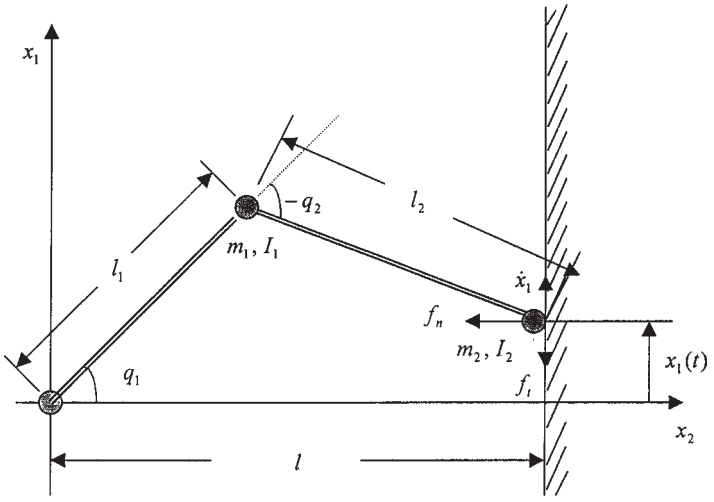

Figure 4. A two-arm robot system.

Table II. Parameters of the controller

g_v	50
g_e	50
Δt	2 ms
δ_1	1.0
δ_2	0.01
Population size	100
Crossover probability	0.98
Mutation probality	0.002
Generations	50

Table III. Initial condition of the manipulator

Link's angular position	$q_1 = 0,$	$q_2 = -\pi/3$
Link's angular velocity	$\dot{q}_1 = 0,$	$\dot{q}_2 = 0$
End effector position	$x_1 = -0.346\,\text{m},$	$x_2 = l = 0.7\,\text{m}$

where the constraint $x_2 = l$ must be satisfied. Clearly, when the end effector is in contact with the surface, x_1 denotes the free motion direction, while along x_2 is the force control direction. The robot is commanded to make sinusoidal movements along the x_1 direction as described by

$$x_1 = -0.346\cos(0.5t), \tag{23}$$

exerting, at the same time, a constant $10Nt$ force along the x_2 direction onto the surface, i.e.,

$$T_\text{d} = 10Nt. \tag{24}$$

It can be expected that $f_{\max}$ in Equation (10) may also be learned with GAs. However, since it learns only at the zero velocity, i.e., at the peak of the sinusoidal movement, the cycle time of learning may be prolonged unendurablly. For simplicity, therefore, $f_{\max}$ is assumed to be exactly known in our simulation. In order to predict its effectiveness and robustness in possible real applications, the following five cases are simulated.

Case 1. No Measurement Noise

The desired dynamic friction coefficients are selected as $\mu = 0.5$ and $\sigma = 2.0$ in this case. A compact set in R^2 must be given within which the GAs search for the pair (μ_e, σ_e) closest to the actual one. Since the robot may be damaged by the normal reaction force due to a large over-compensating force, such a compact set can not be arbitrarily assigned. Moreover, too large a search space may prolong the cycle time of the learning and even degrade its performance. Therefore, in the numerical study, we choose $\Omega \cong [0, 3] \cap [0, 3]$ in the $[\mu, \sigma]$ space for the search.

The typical transient responses of the position x_1 and the force f_n, without and with the learning algorithms being actuated, are shown in Figures 5 and 6, respectively. In Figure 5, the dash lines denote the desired trajectories, while the solid lines are the actual trajectories. Without friction compensation, as can be seen in Figure 5, the friction force causes considerable deviations from the position command and chattering behavior of the force response during velocity reversal. While the normal forces mostly oscillate around the desired one with small amplitudes during the learning process, as can be seen in Figure 6(b). The best-fit value of each generation and the fitness function values v.s. generations are depicted in Figure 7. As can be seen in Figure 7(a), despite the random walks in the first few generations do not follow the actual ones, however, the best-fit values quickly converge to the actual ones after about three generations. The cycle time of the learning for a sampling of 2 ms, as can be easily obtained from Equation (20), is about 0.6 second. It is noted that, the fitness function, as depicted in Figure 7(b), does not always follow the changes of the best-fit values in Figure 7(a) simultaneously. This is mainly due to that the fitness function is evaluated via indirect information of the error signals between the estimated data and the actual ones. Nevertheless, the relative grades within each generation are still very informative and, hence, guides the search efficiently.

Case 2. With Measurement Noise

Since the measurement noises always occur in real systems, we add random noises with zero-mean and amplitudes up to 0.1%, 0.5%, and 0.1% to $x_1, \dot{x}_1, f_n$, respectively. The learning results are shown in Figure 8. Our design is quite robust to small measurement errors. If the noises in f_n increased up to 1%, learning of σ will fail. However, the main contributor of the friction force, i.e., the Coulomb friction force, can still be learned correctly.

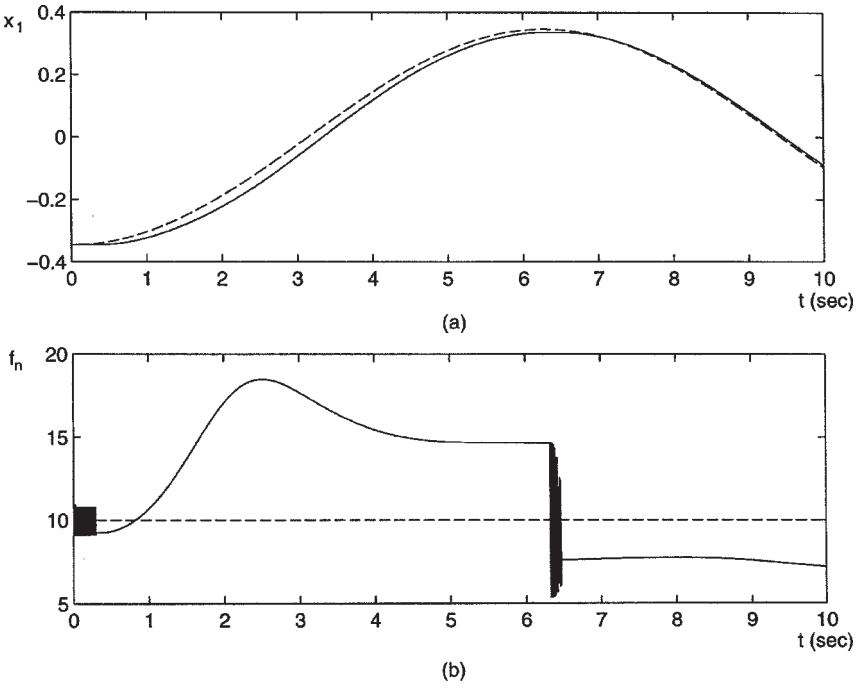

Figure 5. Trajectories without friction compensation.

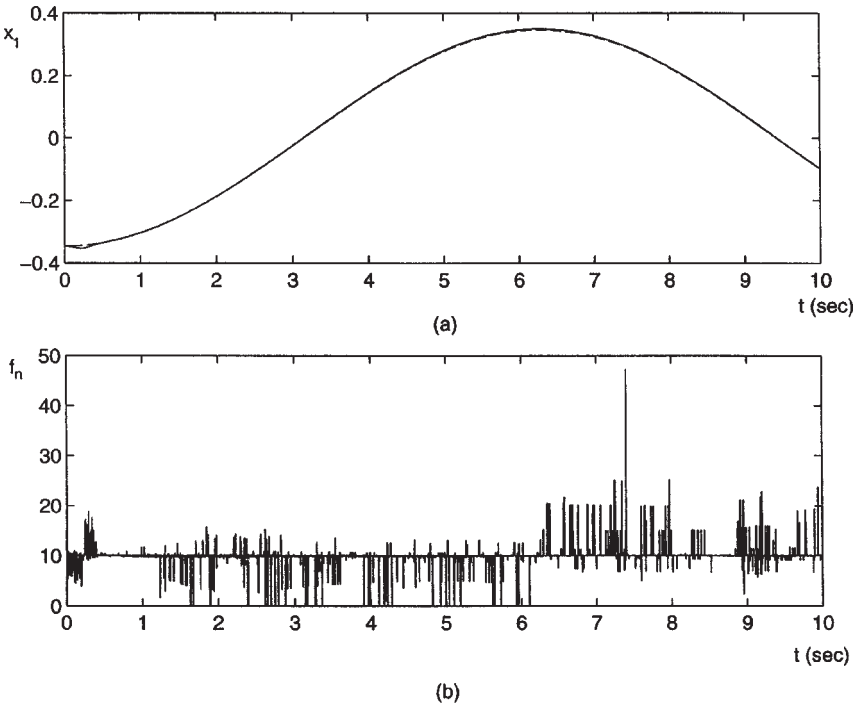

Figure 6. Trajectories during GAs learning.

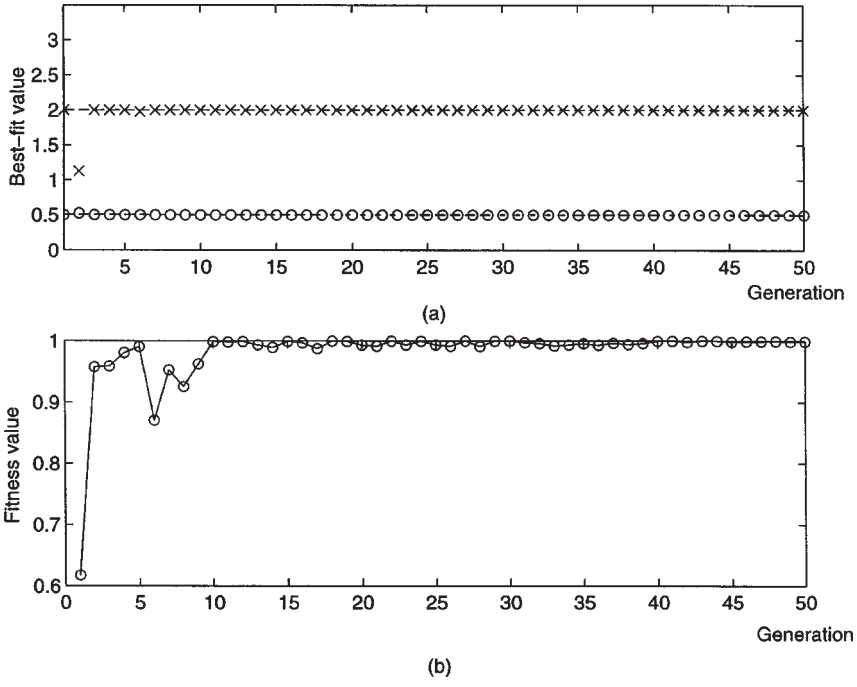

Figure 7. Learning results under perfect circumstances.

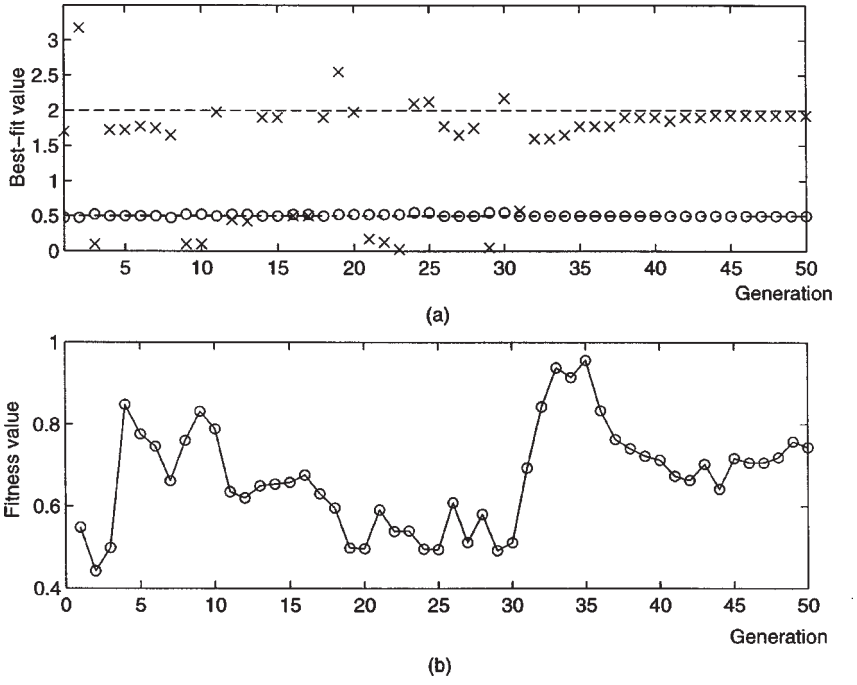

Figure 8. Learning results under small white noises.

Case 3. Friction Models with Stribeck Effect

To predict the effect caused by friction modeling uncertainty, the Stribeck effect exhibited at the low velocity, as depicted in Figure 2(b), is treated as the actual friction model. The model in Equation (12) is adopted to compensate it. We choose $c_1 = 1,\ c_2 = 0.01,\ c_3 = 1$ in Equation (13), which are quite typical, as suggested in [12]. The results are shown in Figure 9. Around the zero velocities, as generations no. 1–5 and 25–35 in Figure 9(a), the disturbance caused by Stribeck effect renders the searching for σ losing directions. However, both friction coefficients can be learned exactly in a later time. This implies that a small uncertainty in the friction modeling such as the Stribeck effect does not affect the final learning results. If a large deviation from the adopted friction model occurs in real applications, large errors of tracking might occur. Even worse, the system might go unstable if without additional force control loop. However, it will not be addressed in this paper.

Case 4. With System Uncertainty

When imperfect cancellation of the nonlinear dynamics occurs in the inner loop of our control design, it can be expected that the residual terms may degrade the performance of the learning. To estimate such an effect, with 1% uncertainty of the term $H(\xi, \dot{\xi})$ in Equation (3) is added to Equations (6), (7) for numerical study. The learning results are shown in Figure 10. As depicted in Figure 10(a), small uncertainty in nonlinear cancellation does not affect the final learning of the actual friction coefficients.

Case 5. Position-Dependent Friction Force

It is known that the friction force could be position-dependent [12]. Therefore, a five-percent amplitude of sinusoidal variations in both μ and σ are added to the target friction model for the numerical study and the GAs are applied to learn these coefficients. The results are shown in Figure 11. The value of μ can still be learned correctly while the learning of σ has totally lost its way. The tracking error, of friction, however, is not significant for the minor role of the viscous term in the total friction. The learning performance is, therefore, regarded as satisfactory.

Finally, during our simulation, we found that small variations in the converging rates and even small deviations from the true coefficients may exist among various experiments. This is mainly owing to the probability-based nature of the genetic algorithm. We also found that no tunings of control parameters are required for learning different friction coefficients [15]. To highlight these, a final simulation with the same numerical values as our first one, except now that μ ranges from 0.1 to 1.0 with step size 0.1 and σ ranges from 0.2 to 2.0 with step size 0.2 took place. The results, of five repetitive runs, for each friction model are given in Table IV. It can be seen that, without tuning of the control parameters, accurate estimation of both friction coefficients can still be easily achieved for quite a large variation of

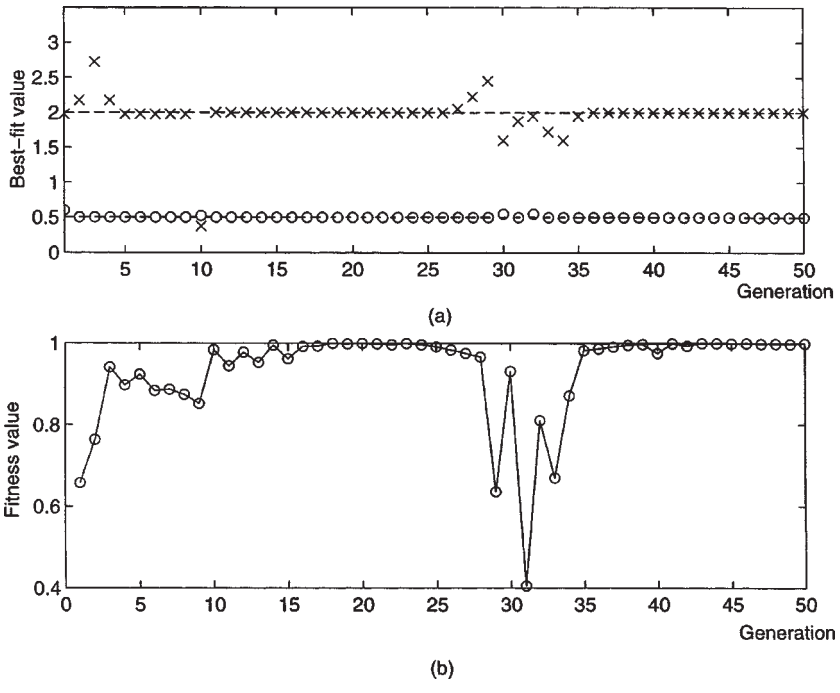

Figure 9. Learning results under friction model uncertainty.

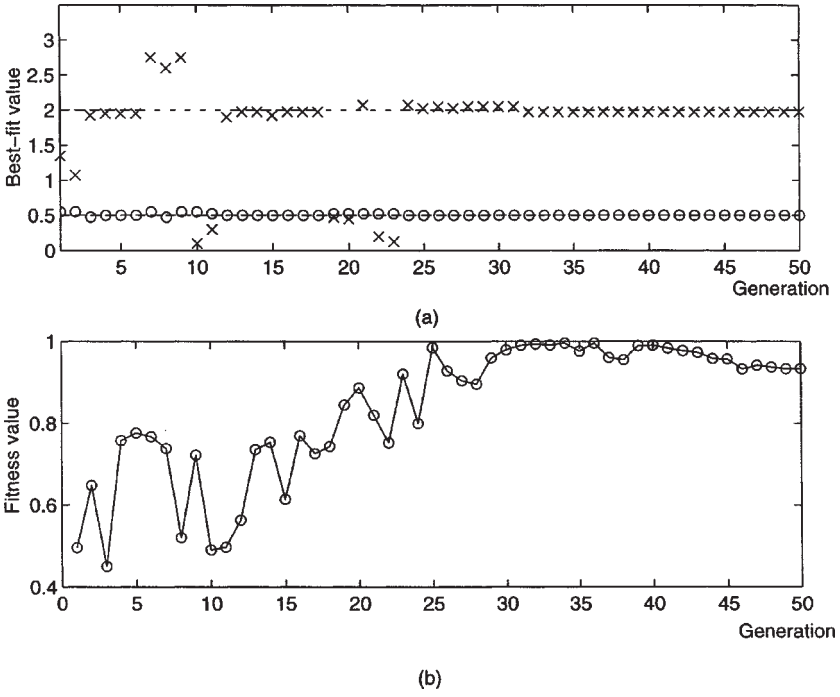

Figure 10. Learning results under imperfect cancellation.

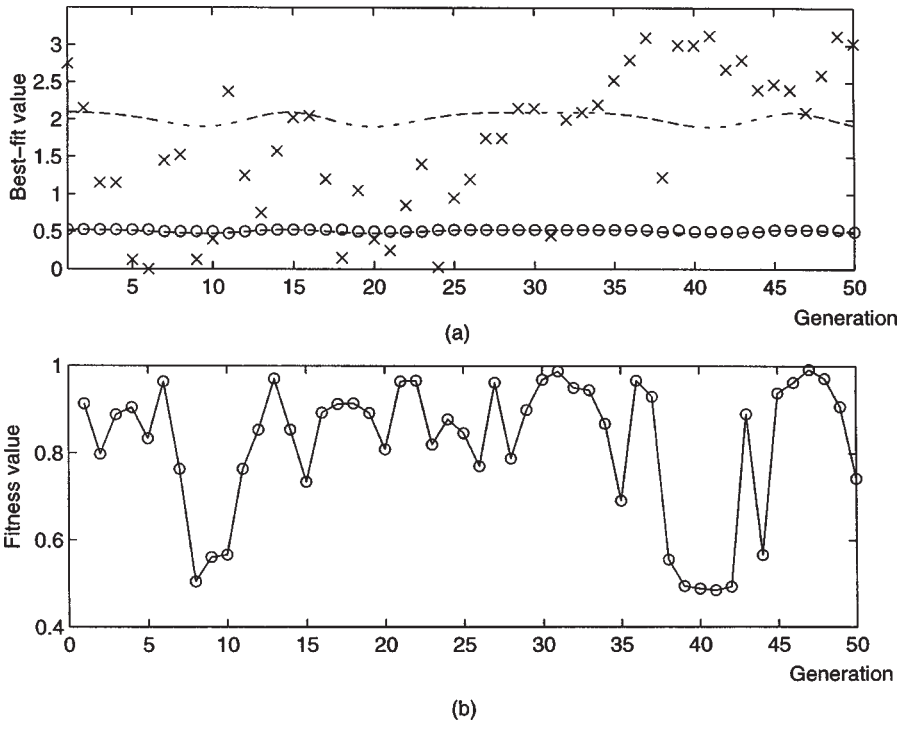

Figure 11. Learning results with position-dependent variations in μ and σ.

Table IV. Results of five repetitive learnings

Friction coefficients	run 1		run 2		run 3		run 4		run 5	
	$\Delta\mu$	$\Delta\sigma$	$\Delta\mu$	$\Delta\sigma$	$\Delta\mu$	$\Delta\sigma$	$\Delta\mu$	$\Delta\sigma$	$\Delta\mu$	$\Delta\sigma$
$\mu = 0.1,\ \sigma = 0.2$	0.000	0.000	0.000	0.000	0.000	0.000	0.000	0.011	0.000	0.000
$\mu = 0.2,\ \sigma = 0.4$	0.000	0.000	0.000	0.085	0.000	0.000	0.000	0.082	0.000	0.000
$\mu = 0.3,\ \sigma = 0.6$	0.000	0.004	0.000	0.008	0.000	0.000	0.000	0.068	0.000	0.011
$\mu = 0.4,\ \sigma = 0.8$	0.000	0.003	0.006	0.105	0.000	0.088	0.000	0.020	0.000	0.019
$\mu = 0.5,\ \sigma = 1.0$	0.000	0.005	0.000	0.007	0.000	0.002	0.000	0.002	0.000	0.006
$\mu = 0.6,\ \sigma = 1.2$	0.000	0.000	0.000	0.000	0.000	0.028	0.000	0.000	0.000	0.023
$\mu = 0.7,\ \sigma = 1.4$	0.000	0.000	0.000	0.002	0.000	0.002	0.000	0.000	0.000	0.002
$\mu = 0.8,\ \sigma = 1.6$	0.000	0.001	0.003	0.058	0.000	0.000	0.000	0.020	0.000	0.000
$\mu = 0.9,\ \sigma = 1.8$	0.000	0.009	0.000	0.000	0.000	0.018	0.000	0.001	0.000	0.003
$\mu = 1.0,\ \sigma = 2.0$	0.000	0.000	0.000	0.001	0.000	0.005	0.000	0.001	0.000	0.001

the actual friction coefficients. The deviations shown in Table IV, denoted as $\Delta\mu$ and $\Delta\sigma$, are defined as

$$\Delta\mu = \sum_{\text{gen}=41}^{50} \frac{|\tilde{\mu}_e(\text{gen}) - \mu|}{10.0} \quad \text{and} \quad \Delta\sigma = \sum_{\text{gen}=41}^{50} \frac{|\tilde{\sigma}_e(\text{gen}) - \sigma|}{10.0},$$

respectively. Here, $\tilde{\mu}_e(\cdot)$ and $\tilde{\sigma}_e(\cdot)$ represent the best estimation in each generation. The deviations thus defined are believed to faithfully reflect the steady-state errors for each test run. Though it seldom occurs, the estimation of σ yields poor accuracy with error up to about twenty percent of the actual ones as can be seen in Table IV. We notice that the viscous force only contributes less than six percent of the total friction in the above simulation. The tracking performance is, therefore, quite acceptable. However, if a higher accuracy is required, a startover of the learning process is suggested to find the actual ones.

5. Concluding Remarks

In this paper, a genetically-based on-line learning compensator is proposed for estimating the two friction coefficients which characterize the friction model for the contact surface. Simulations demonstrate that both coefficients can be quickly and accurately learned within a few seconds. No tuning is required in learning various coefficients over certain ranges. Both position and force trajectories are found to be tracking the desired values after the friction coefficients have been exactly learned.

As shown in simulations, the proposed on-line genetic algorithm design could achieve good friction compensation even under the conditions of measurement noise and system uncertainty. Moreover, from numerical simulations, the proposed control scheme is also found to be feasible for friction compensation of friction model with Stribeck effect and position-dependent friction model.

References

1. Raibert, M. H. and Craig, J. J.: Hybrid position/force control of manipulators, *ASME J. of Dyn. Meas. Control* **103** (1981), 126–133.
2. Khatib, O. and Burdick, J.: Motion and force control for robot manipulators, in: *Proc. of the IEEE Int. Conf. on Robotics on and Automation*, New York, 1986, pp. 1381–1386.
3. Spong, M. and Vidyasagar, M: *Robot Dynamics and Control*, Wiley, New York, 1989.
4. Patarrinski, S. P. and Botev, R. G.: Robot force control: A review, *Mechatronics* **3**(4) (1993), 377–398.
5. McClamroch, N. H. and Wang, D.: Feedback stabilization and tracking of constrained robots, *IEEE Trans. Automat. Control* **33** (1988), 419–426.
6. Jankowski, K. P. and El Maraghy, H. A.: Dynamic decoupling for hybrid control of rigid/flexible-joint robots interacting with the environment, *IEEE Trans. Robotics Automat.* **8**(5) (1992), 519–534.
7. Cai, L. and Song, G.: Joint stick-slip friction compensation of robot manipulators by using smooth robust controllers, *J. Robotic Systems* **11**(6) (1994), 451–470.

8. Yang, S. and Tomizuka, M.: Adaptive pulse width control for precise positioning under the influence of stiction and Coulomb friction, *ASME J. Dyn. Meas. Control* **110** (1988), 221–227.
9. Walrath, C. D.: Adaptive bearing friction compensation based on recent knowledge of dynamic friction, *Automatica* **20**(6) (1984), 717–727.
10. Kubo, T., Anwar, G., and Tomizuka, M.: Application of nonlinear friction compensation to robot arm control, in: *Proc. of the IEEE Int. Conf. on Robotics and Automation*, San Francisco, CA, 1986, pp. 722–727.
11. Kiguchi, K. and Fukuda, T.: Fuzzy neural friction compensation method of robot manipulation during position/force control, in: *Proc. of the IEEE Int. Conf. on Robotics and Automation*, Minneapolis, MN, 1996, pp. 372–377.
12. Armstrong-Hélouvry, B., Dupont, P., and De Wit, C. C.: A survey of models, analysis tools and compensation methods for the control of machines with friction, *Automatica* **30**(7) (1994), 1083–1138.
13. DeJong, K. A.: Adaptive system design: A genetic approach, *IEEE Trans. Systems Man Cybernet.* **SMC-10**(9) (1980), 566–574.
14. Goldberg, D. E.: *Genetic Algorithms in Search, Optimization, and Machine Learning*, Addison-Wesley, Reading, MA, 1989.
15. Varšek, A., Urbančič, T., and Filipič, B.: Genetic algorithms in controller design and tuning, *IEEE Trans. Systems Man Cybernet.* **23**(5) (1993), 1330–1339.
16. Khosla, P. K.: Choosing sampling rates for robot control, in: *Proc. of the IEEE Conf. on Robotics and Automation*, Raleigh, NC, 1987, pp. 169–174.